

Tuning and Hybrid Parallelization of a Genetic-based Multi-Point Statistics Simulation Code

Oscar Peredo^{a,b}, Julián M. Ortiz^{b,c}, José R. Herrero^d, Cristóbal Samaniego^d

^a *Barcelona Supercomputing Center (BSC-CNS), Department of Computer Applications in Science and Engineering, Edificio NEXUS I, Campus Nord UPC, Gran Capitán 2-4, 08034 Barcelona, Catalunya, Spain.*

^b *Advanced Laboratory for Geostatistical Supercomputing, Advanced Mining Technology Center, University of Chile.*

^c *Department of Mining Engineering, University of Chile. Av. Tupper 2069, Santiago, 837-0451, Chile.*

^d *Computer Architecture Department, Universitat Politècnica de Catalunya (UPC-BarcelonaTech), Campus Nord, Mòdul C6, Desp. 206, C/ Jordi Girona 1-3, 08034 Barcelona, Catalunya, Spain.*

Abstract

One of the main difficulties using multi-point statistical (MPS) simulation based on annealing techniques or genetic algorithms concerns the excessive amount of time and memory that must be spent in order to achieve convergence. In this work we propose code optimizations and parallelization schemes over a genetic-based MPS code with the aim of speeding up the execution time. The code optimizations involve the reduction of cache misses in the array accesses, avoid branching instructions and increase the locality of the accessed data. The hybrid parallelization scheme involves a fine-grain parallelization of loops using a shared-memory programming model (OpenMP) and a coarse-grain distribution of load among several computational nodes using a distributed-memory programming model (MPI). Convergence, execution time and speed-up results are presented using 2D training images of sizes $100 \times 100 \times 1$ and $1000 \times 1000 \times 1$ on a distributed-shared memory supercomputing facility.

Keywords: Geostatistics, Stochastic simulation, Multi-point statistics, Code optimization, Parallel computing, Genetic algorithms

1. Multi-point statistics simulation

Numerical modeling with geostatistical techniques aims at characterizing natural phenomena by summarizing and using the spatial correlation of collected data in order to measure the uncertainty at unsampled locations in space. As explained by Deutsch (2002), in simulation techniques, this spatial correlation is imposed into a model commonly constructed on a regular lattice. The models must reproduce the statistical (histogram) and spatial distribution (variogram or other spatial statistics) and their quality is often judged in terms of the reproduction of geological features.

Conventional techniques in geostatistics address the modeling using statistical measures of spatial correlation that quantify the expected dissimilarity (transition to a different category) between locations separated by a given vector distance, in reference to a given attribute, such as the facies, rock type, porosity, grade of an element of interest, among others. This is done using the variogram. Limitations of these techniques have been pointed out in that they only account for two locations at a time when defining the spatial structure (Krishnan and Journel (2003)). Much richer features can be captured by using multi-point statistics (MPS) that consider the simultaneous arrangement of the attribute of interest at several locations, providing the possibility to account for complex features, such as hierarchy between facies, delay effects, superposition or curvilinearity.

MPS simulation aims at generating realizations that reproduce pattern statistics inferred from some training source, usually a training image. For example, in figure 1, left, we can see a training image based on sinuous channels with a simulated realization. These training images are used as a pattern database to generate simulations of the underlying image, as shown in figure 1, right. The simulations use those patterns with the aim that the training and simulated images share the same pattern histogram.

There are several approaches to simulate accounting for MPS. Modifications of conventional methods to impose local directions of continuity using the variogram is a simple approach to impose some of the complex geological



Figure 1: Training image (left) and simulated realization (right)

22 features (Xu (1996); Zanon (2004)). Object based methods and methods inspired in the genetic rules and physics
 23 of the deposition of sediments in different environments also seek to overcome the limitations of conventional cat-
 24 egorical simulation techniques, with significant progress (Deutsch and Wang (1996); Tjelmeland (1996); Pyrcz and
 25 Strebelle (2008)). Presently, the most popular method is a sequential approach based on Bayes' postulate to infer
 26 the conditional distribution from the frequencies of multi-point arrangements obtained from a training image. This
 27 method, originally proposed by Guardiano and Srivastava (1993), and later efficiently implemented by Strebelle and
 28 Journel (2000), is called single normal equation simulation (snesim) (see also Strebelle (2002)). This method has
 29 been the foundation for many variants such as simulating directly full patterns (Arpat and Caers (2007); Eskandari
 30 and Srinivasan (2007)) and using filters to approximate the patterns (Zhang et al. (2006)). The use of a Gibbs Sampling
 31 algorithm to account directly for patterns has also been proposed (Boisvert et al. (2007); Lyster and Deutsch (2008)).
 32 A sequential method using a fixed search pattern and a 'unilateral path' also provides good results (Daly (2005); Daly
 33 and Knudby (2007); Parra and Ortiz (2009)). Other approaches available consider the use of neural networks (Caers
 34 and Journel (1998); Caers and Ma (2002)), updating conditional distributions with multi-point statistics as auxiliary
 35 information (Ortiz (2003); Ortiz and Deutsch (2004); Ortiz and Emery (2005)) or secondary variable (Hong et al.
 36 (2008)). Recently, a couple of new approaches focused on patching patterns directly to reduce computing time and
 37 impose larger scale structures, have been presented (Rezaee et al. (2013); Faucher et al. (2013)). These methods have
 38 a significant potential for practical applications. Alternatively, the problem can be addressed as an optimization one,
 39 using simulated annealing (Deutsch (1992)) or genetic algorithms (Peredo and Ortiz (2012)). The genetic approach is
 40 still under development, but essentially follows the same stochastic strategy as the annealing scheme. This work fo-
 41 cuses on code optimizations and parallelization of a genetic-based sequential code that simulates categorical variables
 42 to reproduce multi-point statistics. However, many of the techniques and ideas proposed here can be applied to other
 43 codes implementing similar simulation algorithms.

44 In section 2 we explain the basic ideas about genetic algorithms, parallel architectures and programming models.
 45 After that, the main bottlenecks of the genetic-based simulation are detailed in section 3. A brief explanation of the
 46 actual implementation is presented in section 4, together with the proposed code optimizations and parallelization
 47 schemes, in sections 5 and 6 respectively. Finally, in the last sections we include the results obtained and final
 48 conclusions.

49 2. Genetic algorithms and Parallel computing

50 Genetic algorithms (GA) were developed in the 1970s with the work of Holland (1975) and in subsequent decades
 51 with De Jong (1980) and Goldberg (1989). Initially used to find good feasible solutions for combinatorial optimization
 52 problems, today they are used in various industrial applications, and recent advances in parallel computing have
 53 allowed their development and continuing expansion.

54 In the canonical approach of GA, typically there is an initial population of individuals, where each individual is

55 represented by a string of bits, as $indiv_k = 000110101$, and a fitness function $fitness(indiv_k)$ which represents the
56 performance of each individual. The fitness function, or objective function, is the objective that must be minimized
57 through the generations over all the individuals. A termination criteria must be defined in order to achieve the desired
58 level of decrement in the fitness function. The main steps and operations performed in a canonical GA can be viewed
59 in algorithm 1. *Selection* and *restart* are operations performed over the entire population. *Selection* extracts the best
60 individuals and *restart* modifies part or the entire population in order to jump from local optimal values. *Crossover*
61 and *mutation* are operations performed over particular individuals of the population. *Crossover* mixes the bits of two
62 individuals according to a predefined set of cut points and *mutation* modifies specific random bits from one individual.
63 Other operators can be found in the mentioned literature.

Algorithm 1 Canonical genetic algorithm

```

1: INPUT:  $N$  individuals (population)
2: Evaluate a fitness function  $fitness$  in each individual
3: while termination criteria is not achieved do
4:   {Breeding a new generation}
5:   Sort the individuals by their fitness function value
6:   if no improvement is measured in the population then
7:     Restart: select some individuals and restart their bits
8:     Sort the individuals by their fitness function value
9:   end if
10:  Selection: select the best individuals based on their fitness function
11:  Crossover: breed new individuals crossing bits of individuals from the selection
12:  Mutation: breed new individuals mutating some bits of individuals from the selection
13:  Replace old individuals with new ones
14:  Evaluate a fitness function  $fitness$  in each individual
15: end while
16: OUTPUT: best individual in the population

```

64 In parallel computing architectures, as described by Culler et al. (1998), the two main models are distributed-
65 memory and shared-memory, with their respective best known programming models MPI (Snir et al., 1998) and
66 OpenMP (Chandra et al., 2001). In the first model, each processor has its own private memory and the data inter-
67 changed between processors travels through a network in chunks of messages. The speed of this communication
68 depends on the speed of the interconnection network. In the second model, each processor has access to a common
69 memory through data coherence and data consistency methods.

70 In order to use efficiently all the resources of parallel architectures, we need to explore algorithms that can exploit
71 the parallelism and be able to adapt to future trends.

72 Genetic algorithms receive the classification of *embarrassingly parallel* technique to solve problems. This clas-
73 sification comes from the fact that separating the workload of the problem into several parallel tasks is trivial. This
74 property motivates its investigation and application in the field of geostatistics, and particularly in MPS simulation.

75 3. Bottlenecks of genetic-based MPS simulation

76 We can see in algorithm 1 that the evaluation of the function $fitness$ is performed $\#generations \times \#individuals$,
77 and strong evidence indicates that this function is the most time consuming routine (a profiling using the `gprof` tool,
78 Graham et al. (2004), tells us that for sufficiently large training images, more than 96% of the execution time is spent
79 in this routine). Its calculation is based on an object called *template*. A *template* T consists in a set of coordinates that
80 defines cell positions. Another interpretation is that a template is basically a pattern of memory accesses. $Patterns(T)$
81 represents all the possible patterns that can be generated from a template T given k possible categories. If a template
82 is defined as $T = \{(1,1), (2,1), (1,2), (2,2)\}$ (4 nodes) and the number of categories is $k = 2$, the pattern database
83 $Patterns(T)$ will have 2^4 elements. Complex geometries can be used to define the template and its corresponding
84 pattern database, for example, in figure 2 we have a template defined as $T = \{(1,1), (5,1), (9,1), (4,4), (5,4), (6,4),$

85 (1,5), (4,5), (5,5), (6,5), (9,5), (4,6), (5,6), (6,6), (1,9), (5,9), (9,9) }. This template is disconnected and its memory-
 86 access pattern is very irregular. This irregularity induces a slowdown in the overall performance when we need to
 87 traverse all its nodes. In contrast, the template of figure 3 has a regular memory-access pattern, if we access to the
 88 first element $T(1, 1)$, additionally the CPU will bring to the cache memory contiguous elements for free (each CPU
 89 has its own cache line size, for example 64 bytes, which means that each cache line can store 16 consecutive integers
 90 of 4 bytes). In Fortran, the CPU will bring a column line, in C/C++, a row line (see Hennessy and Patterson (1990)
 for more details about the CPU memory hierarchy).

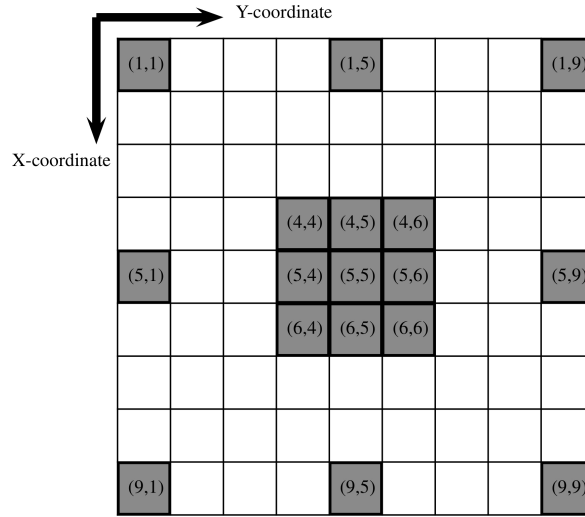


Figure 2: Template of 17 nodes with a complex geometry (irregular memory accesses)

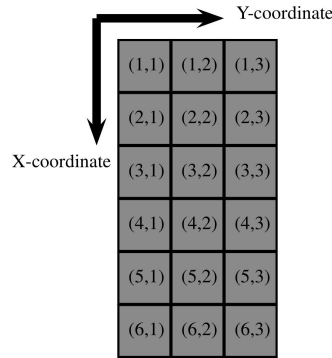


Figure 3: Template of 18 nodes with a simple geometry (regular memory accesses)

91
92
93
94
95
96
97

Given the pattern database $Pattern(T)$, two main tasks must be performed:

- First we have to count the frequency of appearances of each pattern in the training image and store them in an appropriate structure.
- After that, for each individual in the population, and in each generation, we have to count the frequency of appearances of those patterns and calculate the following equation (other possible equations can be viewed in Peredo and Ortiz (2011)):

$$fitness(indiv_k) = \sum_{p \in Patterns(T)} O_p (freq_{Tl}(p) - freq_{indiv_k}(p))^2 \quad (1)$$

with O_p a weight factor for each pattern, $freq_{TI}(p)$ and $freq_{indiv_k}(p)$ the number of appearances of pattern p in a training image and individual $indiv_k$ respectively.

In both tasks, we have to handle with patterns located at boundary nodes. A buffer zone of halo nodes, with size equal to $h = \max\{width(T), height(T)\}$, is added at the boundaries of the training image and realizations. For the training image, an extension of the original image is added keeping the geological continuity and statistical properties (alternative, for sufficiently large images, a reduction of size h in each side of the images can be applied, keeping the removed space as buffer zone). For each individual in the population, the buffer zone is filled with random categorical values between 0 and $k - 1$.

For the first task, following ideas from Straubhaar et al. (2011), we store the frequencies of the patterns that appear in the training image in a list \mathcal{L} . In this list each element is a pair (d, f) where $d = (s_1, \dots, s_{|T|})$ is the pattern (data event), stored as an array of integers of length $|T|$ with $s_i \in \{0, \dots, k - 1\}$ (k categories), and f is the frequency of appearance, stored as an integer. With this structures defined, the algorithm used in this task corresponds to algorithm 2 using an empty frequency list \mathcal{L} .

For the second task, the accounting process is performed using algorithm 2. In this algorithm, we compare the

Algorithm 2 Fitness function calculation: $fitness(indiv_k)$

```

1: INPUT: individual  $indiv_k$ , training image frequency list  $\mathcal{L}$ , template  $T$ 
2:  $sum \leftarrow 0$ 
3:  $\mathcal{L}_{aux} \leftarrow \mathcal{L}$ 
4: for each node  $(i, j)$  from  $indiv_k$  do
5:   Extract pattern located in node  $(i, j)$  using template  $T$  and store it in an array  $localPattern$  of length  $|T|$ 
6:   Search  $localPattern$  in the list  $\mathcal{L}_{aux}$ 
7:   if  $localPattern$  exists in  $\mathcal{L}_{aux}$  then
8:      $\mathcal{L}_{aux}[localPattern] \leftarrow \mathcal{L}_{aux}[localPattern] - 1$ 
9:   end if
10: end for
11: for each pattern  $p$  in  $\mathcal{L}_{aux}$  do
12:    $sum \leftarrow sum + \mathcal{L}_{aux}[p] * \mathcal{L}_{aux}[p]$ 
13: end for
14: OUTPUT:  $sum$ 

```

histograms of the individual and the training image. A considerable bottle-neck for this calculation is the access to the list \mathcal{L} which stores the training image histogram, because for each extracted pattern from an individual, a search must be performed over it in order to see if this pattern exists in the histogram of the training image or not. A proposed solution to this problem is to store the elements (d, f) of the list using a lexicographical order in the patterns d . This order allows to search the existence of a pattern in the list using a binary search with an average and worst case performance of order $O(\log_2 n)$ comparisons, with n the length of \mathcal{L} .

In the next section we will explain the implementation issues for this two tasks using code examples in Fortran 90 as programming language, in order to see the data structures that are used and the proposed optimizations.

4. Implementation

4.1. Storage of pattern frequencies from training image

The routines involved in the storage and management of the list \mathcal{L} are encapsulated in a Fortran module called `patternOperations`. This module consists of a set of global variables and routines performed over arrays of integers. Part of its code structure is depicted in code 1.

```

module patternOperations
  implicit none
  integer(4) :: npatterns

```

```

130 type patternType
131     integer(4), pointer :: pattern(:)
132     integer(4)         :: frequency
133 end type patternType
134 type(patternType), pointer :: patternList(:)
135
136 contains
137     subroutine patternInsertion(...)
138     subroutine patternSearch(...)
139     subroutine patternComparison(...)
140     subroutine printPatternList(...)
141 end module patternOperations
142

```

Code 1: Module patternOperations.f90

144 Initially, when we store the pattern histogram of the training image, we use the global array `patternList` to
145 keep track of the different patterns `patternList(i)%pattern(1:tem_nodes)` with their respective frequencies
146 `patternList(i)%frequency`. A first scan to the training image must be performed in order to fill `patternList`.
147 Using the routine `patternInsertion`, each time a new pattern is found, the memory space used by `patternList` is
148 re-allocated (adding one new element with frequency equal to 1) and all the elements previously inserted together with
149 the new pattern are re-ordered according to a lexicographical order. If an existing pattern is found, the frequencies are
150 updated. The lexicographical order is as follows: given two arrays of integers of the same length $A = (a_1, \dots, a_n)$ and
151 $B = (b_1, \dots, b_n)$ we will say that A is greater than B if and only if $\exists k \in \{1, \dots, n\}$ such that $a_k > b_k$ and $\forall i$ satisfying
152 $i < k$, $a_i = b_i$ holds. For example, given this arrays $A = (0, 0, 0, 1, 0, 0)$ and $B = (0, 0, 0, 0, 0, 0)$, this order will indicate
153 that A is greater than B .

154 After the filling step, `patternList` will be scanned each time we call the routine `patternSearch`. This routine
155 gives the index position in the global array `patternList` where the searched pattern is located, if there is a match. If
156 there is no match, it returns -1. This routine is implemented through a simple iterative binary search, which uses the
157 routine `patternComparison` to compare patterns.

158 The routine `patternComparison` basically traverses each pair of pattern's nodes until they have different values
159 and keeps track of which pattern has the greater one, returning 0 if they are equal, 1 if the first array is *larger* than the
160 second one, and -1 otherwise. The parameters of this routine are two arrays with the pattern values and the length of
161 those arrays (must be equal on both).

162 As we explained before `patternSearch` and `patternComparison` are intensively used by the routine that cal-
163 culates the fitness function. In the worst case, if the training image pattern list \mathcal{L} has size n and the template has t
164 nodes, a search in the list will perform $t \times O(\log_2 n)$ comparisons. For very large templates, this pattern search is very
165 time consuming and different data structures must be used in order to get a reasonable execution time in the search
166 task.

167 4.2. Calculate fitness(indiv_k)

168 Following algorithm 2, which explains all the steps involved in the calculation of the fitness function, in this
169 subsection we explain its associated routine presented in code 2. In this routine, the input `indivk` is a 2D integer
170 array with an image loaded (an *individual* in the genetic algorithm terminology). The inputs `tem_nodes`, `tem_rows`,
171 `tem_cols`, `tem_coord_rows` and `tem_coord_cols` correspond to the specific *template* that we are using. For exam-
172 ple, in figure 2, `tem_nodes = 17`, `tem_rows = tem_cols = 9` and `tem_coord_rows` and `tem_coord_cols` are arrays
173 that store respectively the row and column coordinates of the nodes in template T .

```

174 subroutine fitnessFunction(indivk, rows, cols,
175     tem_rows, tem_cols, tem_nodes,
176     tem_coord_rows, tem_coord_cols, value)
177 use patternOperations !! contains global variables npatterns and patternList
178
179 integer(4), intent(in) :: indivk(rows, cols)
180 integer(4), intent(in) :: rows, cols
181 integer(4), intent(in) :: tem_nodes
182 integer(4), intent(in) :: tem_rows, tem_cols
183 integer(4), intent(in) :: tem_coord_rows(tem_nodes)
184

```

```

185 integer(4), intent(in) :: tem_coord_cols(tem_nodes)
186 integer(4), intent(out):: value
187 integer(4)           :: ii,irow,icol,inode,pos
188 integer(4)           :: freq_aux(npatterns)
189 integer(4)           :: localPattern(tem_nodes)
190
191 do ii=1,npatterns
192     freq_aux(ii)=patternList(ii)%frequency
193 end do
194 value=0
195 do icol = 0,cols-tem_cols
196     do irow = 0,rows-tem_rows
197         do inode = 1, tem_nodes
198             localPattern(inode)=indivk(
199                                     irow+tem_coord_rows(inode),
200                                     icol+tem_coord_cols(inode)
201                                 )
202         end do
203         call patternSearch(tem_nodes,localPattern,pos)
204         if(pos/=-1) then
205             freq_aux(pos)=freq_aux(pos)-1
206         end if
207         end do
208     end do
209 do ii=1,npatterns
210     value=value+freq_aux(ii)*freq_aux(ii)
211 end do
212 end subroutine fitnessFunction
213

```

Code 2: Subroutine fitnessFunction

215 We can see that in this implementation, the values of O_p , the weight factors described in equation (1), are equal to 0
216 if $freq_{TI}(p) = 0$ and equal to 1 otherwise (we only take into account patterns that are present in the training image).

217 5. Code optimization

218 We have applied several code optimization techniques to the previous described routines, in order to better exploit
219 the CPU resources of the sequential execution. These optimizations can be grouped as: increase data locality, improve
220 stack memory usage, code specialization of fitness routine, branch and load reductions.

221 5.1. Increasing data locality of the main data structures

222 The routines patternSearch and patternComparison are based on the global data structure patternList.
223 The first modification consists in adapting this structure to the column-major order of the Fortran language in order to
224 exploit the data and temporal locality.

225 The column-major order in Fortran is related to the way in which the CPU accesses the data stored in memory.
226 In this order, the matrices are accessed using the address $row + (col - 1) * numrows$ with $numrows$ fixed. The cache
227 lines that are moved from the main memory to the cache memory consist in contiguous memory addresses of fixed
228 size. Leaving col fixed and traversing first all values of row , we can minimize the accesses to non-contiguous memory
229 addresses (Hennessy and Patterson (1990)). Modifying the data structures in order to increase this kind of accesses
230 reduces the cache data misses, reducing the overall execution time.

231 The new structure is simply a 2D array in which the row size is the number of nodes in the template, tem_nodes ,
232 and the column size is the number of patterns found in the training image.

```

233 module patternOperations
234     implicit none
235     integer(4) :: npatterns
236     integer(4), pointer :: patternList(:, :) !! (tem_nodes) X (patterns in training image)
237     integer(4), pointer :: frequency(:)    !! (patterns in training image)
238
239

```

```

240 contains
241   subroutine patternInsertion(...)
242   subroutine patternComparison(...)
243   subroutine patternSearch(...)
244   subroutine printPatternList(...)
245 end module patternOperations
246

```

Code 3: Module `patternOperations.f90` with re-designed data structures

248 5.2. Using the stack memory to store local arrays

249 In Fortran, using the Intel's compiler `ifort`, we can use the option `-auto`, which causes all local, non-SAVED
250 variables to be allocated on the run-time stack, including fixed-length arrays. The default is `-auto-scalar`, saving
251 all the scalar variables in the run-time stack. The main advantage is that the access time to the run-time stack is
252 faster than the time access to the run-time heap (which stores the dynamically allocated memory), which decreases
253 the execution time (Intel Corporation (2006)). A negative side of this option is related with the stack size. The stack
254 has a maximum size fixed before the execution and if that size is exceeded, a stack overflow error can be obtained.
255 Also, if we use several threads with OpenMP, each thread has its own stack memory space, so the amount of global
256 stack space is increased proportionally to the number of threads. In order to avoid a stack overflow, we can calculate
257 exactly how much data we need to allocate before compile time and see if it can fit in the stack. If it is too big, we
258 can add more space to the stack, for example using the `ulimit` command in Linux operating systems or setting the
259 environment variable `OMP_STACK_SIZE` with an appropriate value.

260 5.3. Specialization of fitness function to an input template

261 Given an input template, we can specialize our fitness function routine in order to exploit the data accesses pro-
262 vided by the template. For example, in the fitness function of code 2 using the template of figure 2, the variables
263 `icol+1,...,icol+9` are calculated several times, but in reality we only need to calculate them one time per row-
264 iteration and keep their values stored in an auxiliary variable. This allows for avoiding the accesses to the coordinate
265 arrays `tem_coord_rows` and `tem_coord_cols` (see code 4) and keeping the cache memory *clean* for other data.

266 If we denote by $t = \text{tem_nodes}$, $n = \text{cols} - \text{tem_cols}$ and $m = \text{rows} - \text{tem_rows}$, the total number of memory
267 accesses performed by the fitness routine (only taking into account the arrays `tem_coord_rows`, `tem_coord_cols`
268 and `indivk`) is $3 \times t \times n \times m$. Using this optimization the total number of memory accesses for the same arrays
269 is $t \times n \times m$ with a reduction of 3x less memory accesses than the original scenario. In the modified code depicted
270 in 4, using the template described in figure 2, loop unrolling and common subexpression eliminations are included
271 in order to eliminate the accesses of the arrays `tem_coord_rows` and `tem_coord_cols` and re-utilize the values of
272 `icol+1,...,icol+9`.

```

273 subroutine fitnessFunction(...)
274   ...
275   integer(4)::rowplus1,rowplus4,rowplus5,rowplus6,rowplus9
276   integer(4)::colplus1,colplus4,colplus5,colplus6,colplus9
277   ...
278   do icol = 0,cols-tem_cols
279     colplus1=icol+1
280     colplus4=icol+4
281     colplus5=icol+5
282     colplus6=icol+6
283     colplus9=icol+9
284     do irow = 0,rows-tem_rows
285       rowplus1=irow+1
286       rowplus4=irow+4
287       rowplus5=irow+5
288       rowplus6=irow+6
289       rowplus9=irow+9
290       localPattern(1)=indivk(rowplus1,colplus1)
291       localPattern(2)=indivk(rowplus5,colplus1)
292       localPattern(3)=indivk(rowplus9,colplus1)
293

```



```

294     ...
295     localPattern(15)=indivk(rowplus1,colplus9)
296     localPattern(16)=indivk(rowplus5,colplus9)
297     localPattern(17)=indivk(rowplus9,colplus9)
298     call patternSearch(tem_nodes,localPattern,pos)
299     if(pos/=-1) then
300         freq_aux(pos)=freq_aux(pos)-1
301     end if
302 end do
303 end do
304 ...
305 end subroutine fitnessFunction
306

```

Code 4: Subroutine fitnessFunction specialized to the input template of figure 2

308 5.4. Branch reduction

309 The routine patternComparison, described in code 5, which is the most intensive in terms of execution time,
310 can be re-designed in order to reduce the number of branch instructions (control flow, for example if-then-else or
311 while loops) executed inside a loop.

```

312 subroutine patternComparison(length,onePattern1,onePattern2,value)
313 !
314 ! Compare two patterns.
315 ! If value = 0, both patterns are equals
316 ! If value = 1, the first pattern is bigger
317 ! If value = -1, the second pattern is bigger
318 !
319 integer(4), intent(in) :: length
320 integer(4), intent(in) :: onePattern1(length)
321 integer(4), intent(in) :: onePattern2(length)
322 integer(4), intent(out) :: value
323 integer(4) :: ii
324
325 value = 0
326 ii = 0
327 do while ( value == 0 .and. ii < length )
328     ii = ii + 1
329     if ( onePattern1(ii) > onePattern2(ii) ) then
330         value = 1
331     elseif ( onePattern1(ii) < onePattern2(ii) ) then
332         value = -1
333     end if
334 end do
335 end subroutine patternComparison
336
337

```

Code 5: Subroutine patternComparison

339 When a branch instruction is processed by the CPU, some cycles may be lost due to an incorrect branch prediction
340 or an expensive condition evaluation (Hennessy and Patterson (1990)). For that reason, we know that reducing the
341 number of branches and relaxing their boolean conditions are good practices in order to reduce the overall execution
342 time. A first version of the modified routine can be viewed in code 6.

```

343 subroutine patternComparison(length,onePattern1,onePattern2,value)
344 ! Compare two patterns.
345 ! If value = 0, both patterns are equals
346 ! If value = 1, the first pattern is bigger
347 ! If value = 2, the second pattern is bigger
348 integer(4), intent(in) :: length
349 integer(4), intent(in) :: onePattern1(length)
350 integer(4), intent(in) :: onePattern2(length)
351 integer(4), intent(out) :: value
352

```

```

353 integer(4)          :: ii
354 value = 0
355 ii = 0
356 do while ( value == 0 .and. ii <length )
357     ii = ii + 1
358     value=onePattern1(ii) - onePattern2(ii)
359 end do
360 end subroutine patternComparison
362

```

Code 6: First re-design of subroutine `patternComparison` with reduced number of branch instructions

363 In this re-design, almost all the branch instructions were eliminated from the original routine. Only the ones
364 injected in the boolean conditions of the `while` loop remain. One possible way to get rid of the evaluation of those
365 conditions is to unroll the loop and use explicit evaluations of each statement incrementing the value of the variable
366 `ii`. Using this technique we are avoiding conditional evaluations and reducing the number of branch instructions
367 performed by the CPU. The re-designed routine can be viewed in code 7. This modified routine is specialized and
368 depends on the number of nodes of the template. In this case we are using the template described in figure 2.

```

369
370 subroutine patternComparison(length,onePattern1,
371                             onePattern2,value)
372     integer(4), intent(in)    :: length
373     integer(4), intent(in)    :: onePattern1(length)
374     integer(4), intent(in)    :: onePattern2(length)
375
376     value=onePattern1(1) - onePattern2(1)
377     if (value/=0) return
378     value=onePattern1(2) - onePattern2(2)
379     if (value/=0) return
380     ...
381     value=onePattern1(16) - onePattern2(16)
382     if (value/=0) return
383     value=onePattern1(17) - onePattern2(17)
384     if (value/=0) return
385 end subroutine patternComparison
388

```

Code 7: Second re-design of subroutine `patternComparison` with reduced number of branch instructions and minimal boolean conditionals

388 5.5. Load reduction

389 In the previous optimized routine `patternComparison` (code 7) the value of the array `onePattern2` is invariant
390 through the entire execution of the caller routine `patternSearch`, implemented as depicted in code 8.

```

391
392 subroutine patternSearch(length,onePattern,pos)
393     !
394     ! Search a pattern in the pattern
395     ! database of training image
396     ! If pos!=-1, found
397     ! If pos==-1, not found
398     !
399     use patternOperations      !! contains global variables npatterns and patternList
400     integer(4), intent(in)    :: length
401     integer(4), intent(in)    :: onePattern(length)
402     integer(4), intent(out)   :: pos
403     integer(4)                :: isFound,minn,maxx
404     integer(4)                :: value,ii,jj
405
406     minn = 1
407     maxx = npatterns
408     isFound=0
409     do while ( minn <= maxx .and. isFound == 0 )
410         pos = int(real(minn+maxx)* 0.5)
411         call patternComparison(

```

```

412         length,
413         patternList(pos)%pattern,
414         onePattern,
415         value
416     )
417     if (value == 0) then
418         isFound = 1
419     elseif (value == 1) then
420         maxx = pos - 1
421     else
422         minn = pos + 1
423     end if
424 end do
425 if (isFound == 0) pos = -1
426 end subroutine patternSearch
428

```

Code 8: Subroutine patternSearch

429 Its values correspond to the pattern that is going to be searched in the pattern database stored in patternList.
430 Storing each of the array cells in register variables (up to the maximum number of integer registers available in the
431 CPU) is an alternative that reduces the number of loads performed by the CPU. The variables op1 to op17 store the
432 values of onePattern(1) to onePattern(17), using the template of figure 2. Using a pseudo-inlined version of
433 the routine patternComparison together with the registers op1 to op17 allows us to reduce by a half the number
434 of loads executed and also to reduce completely the number of routine calls to patternComparison. The code 9
435 depicts this modifications.

```

436
437
438
439
440
441
442
443
444
445
446
447
448
449
450
451
452
453
454
455
456
457
458
459
460
461
462
463
464
465
466
467
468
469
470
471
472
473

```

```

subroutine patternSearch(length,onePattern,pos)

    use patternOperations    !! contains global variables npatterns and patternList

    integer(4), intent(in)  :: length
    integer(4), intent(in)  :: onePattern(length)
    integer(4), intent(out) :: pos
    integer(4)              :: isFound
    integer(4)              :: minn,maxx,value
    integer(4)              :: ii,jj,pos
    integer(4)              :: op1,op2,op3,op4
    ...
    integer(4)              :: op15,op16,op17

    op1=onePattern(1)
    ...
    op17=onePattern(17)
    minn = 1
    maxx = npatterns
    pos = -1
    do while ( minn <= maxx )
        pos = int(real(minn+maxx)* 0.5)
        do
            value=patternList(1,pos) - op1
            if(value/=0)exit
            ...
            value=patternList(17,pos) - op17
            if (value/=0)exit
            exit !! value==0
        end do
        if (value == 0) then
            minn = maxx + 1
        elseif (value == 1) then
            maxx = pos - 1
        else
            minn = pos + 1
        end if
    end while
end subroutine patternSearch

```

```

474   end do
475 end subroutine patternSearch
476

```

Code 9: Re-design of subroutine `patternSearch` with reduced number of loads

478 6. Parallelization

479 6.1. Fine grained parallelization with OpenMP

480 A parallelization scheme using OpenMP over a genetic-based MPS code was described in Peredo and Ortiz (2012).
481 In that work, the proposed parallelization was based on parallel do-loops over the fitness function routine. The
482 parallelization presented in this work is essentially the same, based on parallel do-loops, but taking in consideration
483 the previously described code optimizations.

```

484
485 subroutine fitnessFunction(...)
486   use patternOperations
487   ...
488   idthread=omp_get_thread_num()+1
489   numthreads=omp_get_num_threads()
490   ...
491   do ii=1,npatterns
492     freq_aux(ii)=frequency(ii)      !! global
493     freq_aux_by_id(ii,idthread)=0   !! local
494   end do
495   value=0
496
497   !$OMP PARALLEL PRIVATE( localPattern,pos,icol,irow, &
498   !$OMP colplus1,colplus4,colplus5,colplus6,colplus9, &
499   !$OMP rowplus1,rowplus4,rowplus5,rowplus6,rowplus9, &
500   !$OMP freq_aux_by_id )
501   !$OMP DO
502   do icol = 0,cols-tem_cols
503     colplus1=icol+1
504     colplus4=icol+4
505     colplus5=icol+5
506     colplus6=icol+6
507     colplus9=icol+9
508     do irow = 0,rows-tem_rows
509       localPattern(1)=indivk(rowplus1,colplus1)
510       ...
511       localPattern(17)=indivk(rowplus9,colplus9)
512       call patternSearch(tem_nodes,localPattern,pos)
513       if(pos/=-1) then
514         freq_aux_by_id(pos,idthread)=freq_aux_by_id(pos,idthread) + 1
515       end if
516     end do
517   end do
518   !$OMP END DO
519   !$OMP END PARALLEL
520
521   do jj=1,numthreads
522     do ii=1,npatterns
523       freq_aux(ii)=freq_aux(ii)-freq_aux_by_id(ii,jj)
524     end do
525   end do
526
527   do ii=1,npatterns
528     value=value+freq_aux(ii)*freq_aux(ii)
529   end do
530 end subroutine fitnessFunction
531

```

Code 10: Parallelization of specialized subroutine `fitnessFunction` with OpenMP

533 The main difference with the sequential code 2, besides the code optimizations, is the utilization of a local array
 534 `freq_aux_by_id` which stores the frequencies of the patterns calculated locally by all threads. After each thread
 535 finishes their corresponding loops (an implicit wait is placed at the end of the loop for thread synchronization) all
 536 those frequencies are gathered into the global array `freq_aux` and this array is used to calculate the final value of the
 537 fitness function.

538 Several schedules (`static`, `dynamic` and `guided` with different chunk sizes) were tested but none of them was
 539 considerably faster than the others, so we choose to stay using the `static` schedule in all of our tests. No profit was
 540 obtained after tuning the chunk size, because no false sharing (a review of this topic can be found in Culler et al.
 541 (1998)) was introduced in the calculations since no writing is done in the matrix `indivk`. The default value of chunk
 542 size was used in the execution of the tests.

543 6.2. Coarse grained parallelization with MPI+OpenMP

544 If the initial population is distributed in several processes, the amount of work that each process does decreases
 545 with a reduction in the execution time. Following ideas from Cantú-Paz (1998), we implement an *island-based*
 546 parallelization scheme in which each process waits for the best individuals calculated by the others (other *islands*),
 547 and asynchronously each process sends to everybody the best individual calculated by itself. In this way, all processes
 548 share the same best individuals and each one can combine them in order to breed a new generation. The steps are
 549 depicted in algorithm 3. Using this distribution of load, each process can use several threads with OpenMP as in the
 550 previous subsection and the code optimizations explained in the previous section. The result of this integration is a
 551 hybrid distributed-shared memory parallelization based on the MPI and OpenMP programming models.

Algorithm 3 Parallel canonical genetic algorithm (based on island model)

```

1: INPUT:  $P$  processes,  $\frac{N}{P}$  individuals per process (population)
2: for each process  $p$  do
3:   Evaluate a fitness function  $fitness$  in each individual
4:   while termination criteria is not achieved do
5:     {Breed a new generation}
6:     Sort the individuals by their fitness function value
7:     if no improvement is measured in the local population then
8:       Restart: select some individuals and restart their bits
9:       Sort the individuals by their fitness function value
10:    end if
11:    Selection: select the best individuals based on its fitness functions
12:    Crossover: breed new individuals crossing bits of individuals from the selection
13:    Mutation: breed new individuals mutating some bits of individuals from the selection
14:    Replace old individuals by new ones
15:    Send (asynchronously) the best individual to the other processes
16:    Receive (asynchronously) the best individuals from other processes and copy them in the population (using
    the memory space of the worst individuals)
17:    Evaluate a fitness function  $fitness$  in each individual
18:  end while
19: end for
20: OUTPUT: best individual in population of process master.

```

552 The only drawback of this parallel implementation is the reduction of the population size in each island. Each
 553 process will have a population of $\frac{N}{P}$ individuals, and if N is not sufficiently large, local minimum will be achieved
 554 earlier in the convergence process, restricting the search for better solutions. A solution to this problem is to set large
 555 population sizes according to the number of processes involved in the executions and the size of the search space,
 556 in our case, the number of template nodes and training image nodes. Several tests must be done in order to get a
 557 good estimation of the optimal population size. In this work, however, our focus was to get reasonable values of
 558 performance and convergence, leaving this topic for future research.

559 The key part of the parallel strategy is the communication between the processes, which is equivalent to an all-to-
 560 all broadcast of the best individuals stored in each island. This communication can be implemented with MPI using
 561 asynchronous MPI_Isend/MPI_Irecv/MPI_Wait or with the intrinsic routine MPI_Allgather.

562 A performance analysis tool called Paraver, described in Labarta et al. (1995), was used to generate trace views
 563 associated to an execution of the proposed implementation using 16 processes with 1 and 12 threads each. In these
 564 traces we can see the different states of execution described in algorithm 3. In the X-axis we have the execution time
 565 in microseconds and in the Y-axis we have the states of processes and threads. In figure 4 we can see the overall
 566 execution time with both processors sets using the same time scale.

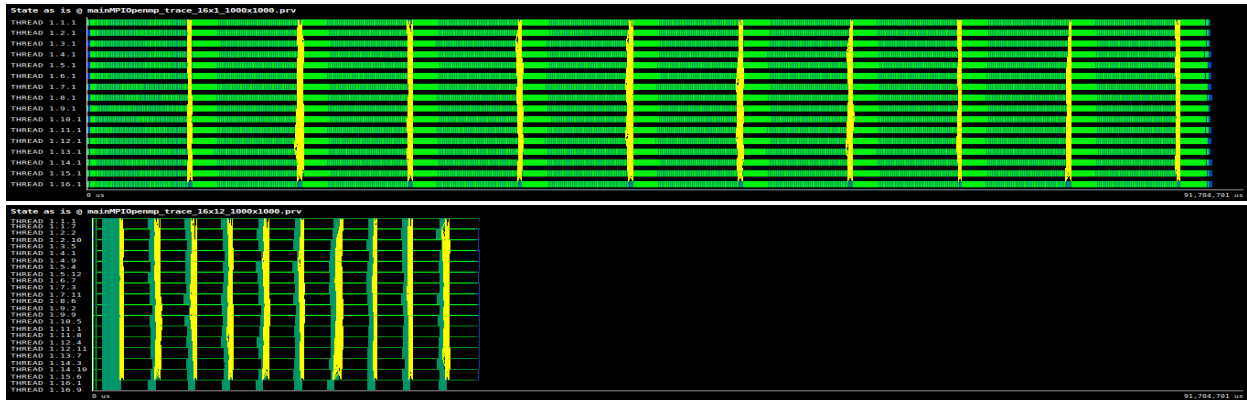


Figure 4: Execution trace (using the same time scale) with two processor sets, 16x1 (top) and 16x12 (bottom) processesxthreads, using a training image of size 1000x1000 running 10 generations of the algorithm 3

567 7. Results

568 7.1. Timing

569 In order to study the effectiveness of the optimizations and parallelizations, we use a test routine which loads two
 570 2D images, using one as training image and the other one as individual. After that, it calculates the fitness function of
 571 the individual using the previous routines. All measurements are average of 100 executions of this test routine. Two
 572 images sizes were used, 100 x 100 and 1000 x 1000. They are shown in figure 5. Additionally, full iterations were
 573 measured running 30 generations of the genetic algorithm.

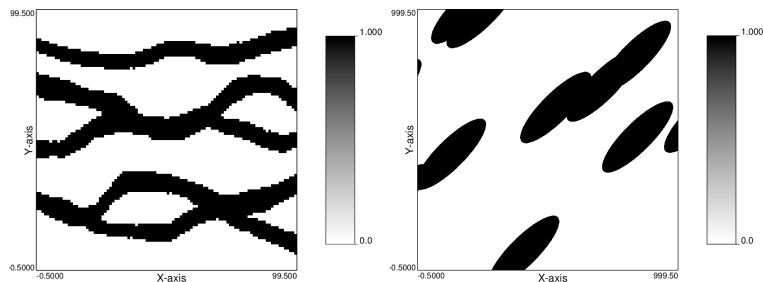


Figure 5: Training images of size 100x100 (left) and 1000x1000 (right)

574 The code optimizations were tested incrementally: if an optimization X reduces the execution time, all the subse-
 575 quent optimizations are calculated over the baseline time using the optimization X. The code compilation was done
 576 using ifort (Intel Fortran Compiler) version 12.0.4 (20110427) (Intel Corporation (2011)), without any added op-
 577 tions or flags. The default level of compiler optimization is -O2. The tests were executed in a cluster of compute nodes

578 running Linux operating system where every node has two processors Intel Xeon E5649 6-Core (12 CPUs per node)
 579 at 2.53 GHz with 24 GB of RAM memory, 12MB of cache memory and 250 GB local disk storage. The execution
 580 times and speed-up values obtained is detailed in tables 1 to 5.

| Optimization | 100×100 | | 1000×1000 | |
|---------------------------|----------------|----------|----------------|----------|
| | Time (seconds) | Speed up | Time (seconds) | Speed up |
| Baseline | 0.00319 | 1 | 0.402347 | 1 |
| Increase data locality | 0.00213 | 1.49x | 0.26368 | 1.53x |
| Use Stack memory | 0.00208 | 1.53x | 0.257903 | 1.56x |
| Specialization of fitness | 0.00181 | 1.76x | 0.243201 | 1.65x |
| Branch reduction | 0.00160 | 1.99x | 0.222511 | 1.80x |
| Load reduction | 0.00157 | 2.03x | 0.214222 | 1.87x |

Table 1: Code optimization: fitness function calculation of a 100×100 and 1000×1000 images using the template in figure 2

581

| Threads | 100×100 | | 1000×1000 | |
|---------|----------------|----------|----------------|----------|
| | Time (seconds) | Speed up | Time (seconds) | Speed up |
| 1 | 0.003190 | 1x | 0.402347 | 1x |
| 2 | 0.001800 | 1.77x | 0.186401 | 2.15x |
| 4 | 0.031770 | 0.10x | 0.094410 | 4.26x |
| 6 | 0.020684 | 0.15x | 0.065002 | 6.18x |
| 8 | 0.027191 | 0.11x | 0.055411 | 7.26x |
| 10 | 0.046754 | 0.06x | 0.049403 | 8.14x |
| 12 | 0.027156 | 0.11x | 0.037000 | 10.87x |

Table 2: Fine-grained parallelization without code-optimizations: fitness function calculation of a 100×100 and 1000×1000 images using the template in figure 2

582

| Threads | 100×100 | | 1000×1000 | |
|-------------|----------------|----------|----------------|----------|
| | Time (seconds) | Speed up | Time (seconds) | Speed up |
| 1 | 0.003190 | 1x | 0.402347 | 1x |
| 1+code-opt | 0.001573 | 2.03x | 0.222202 | 1.80x |
| 2+code-opt | 0.002028 | 1.57x | 0.109205 | 3.68x |
| 4+code-opt | 0.012321 | 0.25x | 0.056436 | 7.12x |
| 6+code-opt | 0.015411 | 0.20x | 0.041220 | 9.76x |
| 8+code-opt | 0.027145 | 0.11x | 0.036421 | 11.04x |
| 10+code-opt | 0.016694 | 0.19x | 0.030886 | 13.02x |
| 12+code-opt | 0.017766 | 0.17x | 0.023531 | 17.09x |

Table 3: Fine-grained parallelization with code-optimizations: fitness function calculation of a 100×100 and 1000×1000 images using the template in figure 2

583

584

585

586 Based on the results from table 1, the code optimization accelerates considerably the sequential execution of the
 587 fitness function calculation. A speedup of 2.03x and 1.87x was obtained for images of 100×100 and 1000×1000
 588 respectively. The best results were obtained after re-designing the data structures that handle the pattern list, allowing
 589 it to reduce the execution time by improving the locality of the memory accesses.

| Processes×Threads | 100×100 | | Processes×Threads | 1000×1000 | |
|-------------------|----------------|----------|-------------------|----------------|----------|
| | Time (seconds) | Speed up | | Time (seconds) | Speed up |
| 1×1 | 3.466 | 1x | 1×1 | 312.133 | 1x |
| 1×2 | 1.852 | 1.87x | 1×12 | 55.62 | 5.61x |
| 2×2 | 0.934 | 3.71x | 2×12 | 27.53 | 11.33x |
| 4×2 | 0.556 | 6.23x | 4×12 | 14.03 | 22.24x |
| 8×2 | 0.295 | 11.74x | 8×12 | 7.26 | 42.99x |
| 16×2 | 0.213 | 16.27x | 16×12 | 4.02 | 77.64x |

Table 4: Coarse-grained parallelization without code optimizations: average generation step (30 generations) of the genetic algorithm using a population of 1000 individuals, each one a 100×100 and 1000×1000 images respectively, using the template in figure 2

| Processes×Threads | 100×100 | | Processes×Threads | 1000×1000 | |
|-------------------|----------------|----------|-------------------|----------------|----------|
| | Time (seconds) | Speed up | | Time (seconds) | Speed up |
| 1×1 | 3.466 | 1x | 1×1 | 312.133 | 1x |
| 1×1+code-opt | 2.032 | 1.70x | 1×12+code-opt | 42.911 | 7.10x |
| 2×1+code-opt | 1.027 | 3.37x | 2×12+code-opt | 22.102 | 14.12x |
| 4×1+code-opt | 0.561 | 6.17x | 4×12+code-opt | 11.354 | 27.49x |
| 8×1+code-opt | 0.310 | 11.18x | 8×12+code-opt | 5.916 | 52.76x |
| 16×1+code-opt | 0.221 | 15.68x | 16×12+code-opt | 3.085 | 101.17x |

Table 5: Coarse-grained parallelization with code optimizations: average generation step (30 generations) of the genetic algorithm using a population of 1000 individuals, each one a 100×100 and 1000×1000 images respectively, using the template in figure 2

590 According to the results from tables 2 and 3, the fine-grain parallelization allows to accelerate the execution
591 considerably only when the size of the training image and realizations are large, in our case a size of 1000×1000
592 reaching a speedup of 17.09x with 12 threads in the best case. With a size of 100×100 no profit from the parallelization
593 was observed (except in the non-optimized code with 2 threads), due to the small amount of work that each thread
594 performs compared with the overhead introduced by thread management. The best speedup result, 2.03x, was obtained
595 using the optimized code with only one thread.

596 The coarse-grain parallelization accelerates the execution proportionally to the number of processes involved in
597 it. This feature is obtained after distributing the workload evenly among the processes. In our case, the workload is
598 represented by the population, which is divided among the processes. According to tables 4 and 5, the best results
599 achieved in terms of speedup were obtained using the hybrid parallelization scheme with optimized code, MPI and
600 OpenMP on large training and realization images of size 1000×1000. The thread selection policy used to defined how
601 many threads will run in each test was based in the best results obtained in the corresponding fine-grain tests from
602 tables 2 and 3, namely, 2 and 12 threads for small and large images respectively, using non-optimized code, and 1 and
603 12 threads for small and large images respectively, using optimized-code.

604 7.2. Convergence

605 In order to test the convergence of the method using the parallel optimized code, we choose a fixed set of param-
606 eters for the genetic algorithm and with those parameters we observe the behaviour of the fitness function and the
607 realization obtained, starting from a randomly generated population of individuals. Those parameters are:

- 608 • population size: 640 individuals
- 609 • mutation rate: described in the next paragraph
- 610 • crossover percentage: 50%, corresponding to the number of individuals selected to perform a crossover with
611 other individual
- 612 • restart percentage: 10%, corresponding to the percentage of individuals that will be restarted, in each restart
613 step
- 614 • number of cut-points: 10%, corresponding to the number of cut-points in the crossover operation
- 615 • number of mutation nodes: described in the next paragraph

616 In order to accelerate the convergence, a multi-point mutation strategy was implemented. In this strategy, a
 617 random node and a random category were selected (in our tests, we have only 2 categories). Using an influence radius
 618 r calculated a priori (in our case $r = 0.02 \times \min(\#rows, \#columns)$) all nodes that fall within the circle centered in
 619 the random node with radius r are *mutated* (changed) into a new selected category (leaving the conditionant nodes
 620 without modification). Additionally, a cyclic-cooling scheme was implemented in order to control the variability of
 621 the population, by means of reducing the mutation ratio by a factor $\lambda \in (0, 1)$ each 1000 generations. Starting from a
 622 mutation rate $m = 1$, if λm goes below a threshold, the ratio is restarted from $m = 1$ and a new mutation cycle begins.

623 Samples of realization images and convergence plots of function 1 are included in figures 6-7. The convergence
 624 plots show the relative decrease in percentage of the fitness function with respect to the initial value (the best fitness
 625 value obtained in the first population of individuals). As we can see in these figures, the simulated images are not equal
 626 to the training image, which is not bad, because one of the objectives of the simulation process using MPS methods
 627 is to obtain simulated images that fits the underlying statistics of the training image but not being necessarily equal.
 628 If conditional data is used (nodes with information from the training image which are not modified in the simulation
 629 process) the resulting simulated image will be more similar to the training image with the corresponding match of
 630 the underlying statistics. The tests that we are considering do not use any conditional data. Therefore they must be
 631 considered as a worst case scenario in terms of convergence.

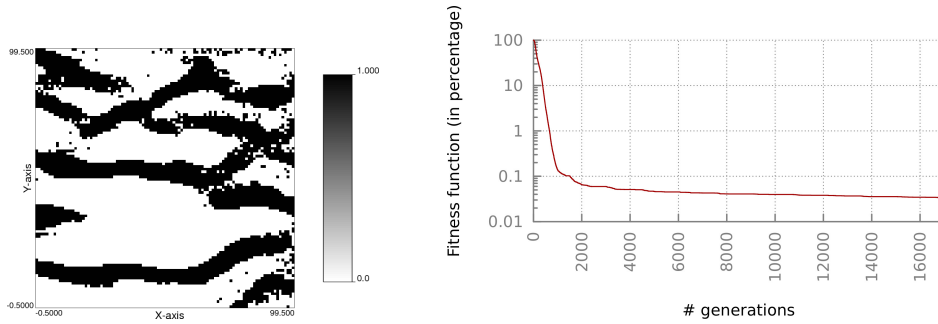


Figure 6: Simulated realization of size 100x100 (left) and convergence plot showing 17000 generations

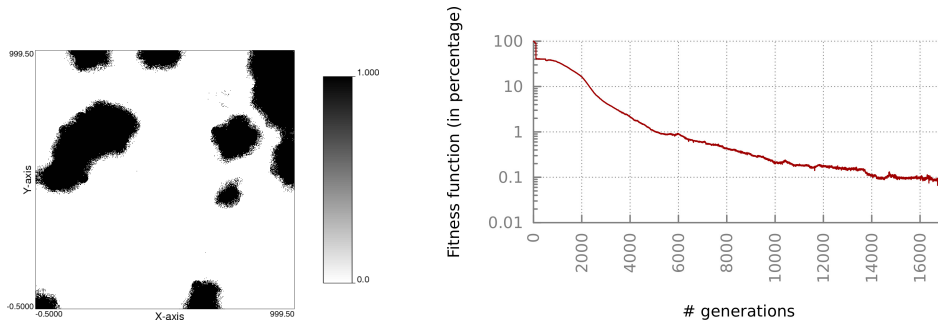


Figure 7: Simulated realization of size 1000x1000 (left) and convergence plot showing 17000 generations

632 8. Conclusions

633 The proposed hybrid parallelization using an optimized code has shown reasonable speedup results, according to
 634 the time measurements reported in section 7. The differences between non-optimized and optimized code execution
 635 are considerable and justify our research in this recent topic. A negative aspect has to do with the loss of generality
 636 of some of the proposed optimizations. Applying routine specialization or branch/load reduction introduces several

637 modifications in the corresponding code, were specific values of the size of the template are used. If the size or
638 geometry of the template changes, we need to modify those routines in order to adapt them to the new template's
639 values. If the complete code has to be used in an agile framework allowing the utilization of user-defined templates,
640 this behaviour can generate inconveniences because each new template needs its own optimized routines, with their
641 corresponding creation, compilation and inclusion in the main application. A possible solution to this problem can be
642 the adoption of auto-tuning techniques to automatically deploy new kernels according to the geometry of the template
643 in use. Examples of auto-tuning techniques applied to stencil optimization for Finite Differences PDE solvers can be
644 reviewed in Datta et al. (2008, 2009).

645 The strategies proposed to accelerate the convergence allow us to get fast realizations, using reasonable small
646 populations (40 individuals per process) and a small restart percentage (10% of the population is restarted). However,
647 a further research on the acceleration of convergence by tuning the genetic parameters (population size, mutation
648 and crossover rates, percentage of selection, percentage of restarted population, number of cross points and mutation
649 points, among others) is left open for future research. Also, several other research topics can be explored, among
650 them we can mention: dynamic mutation rate (using the full annealing scheme), non-linear crossovers (using external
651 information to mix two realizations with some physical or geological interpretation), or selective restart (allowing to
652 reset only individuals that meet certain properties).

653 This work focuses on 2D training images and realizations. However 3D models are used in real geostatistical
654 scenarios. In order to adapt our code to the 3D scenario, several further optimizations and modifications must be
655 done, but these are left as future work. Among the most relevant ones we can mention the specialization of the
656 fitness evaluation to 3D templates, use of efficient data structures to manage large 3D images and 1D individuals,
657 new methods to perform crossover and mutations in these individuals, and modifications of the fine and coarse grain
658 strategies to the new 3D scenario. Another related future work could be the application of the fitness calculation
659 optimized routines into the simulated annealing scheme of simulation as described in Deutsch (1992), using the MPI
660 implementation described in Peredo and Ortiz (2011) or the standard routines implemented in the GSLIB library from
661 Deutsch and Journel (1992).

662 Finally, another possible research area is related to explore new computer architectures with this algorithm. Among
663 the possible alternatives are NVIDIA's GPUs (using two programming models, CUDA and OpenACC), Intel's MICs
664 (several cores in one chip and accelerators working together in Intel architectures) or energy-efficient new supercom-
665 puters that will be available in the next years.

666 References

- 667 Arpat, B., Caers, J., 2007. Stochastic simulation with patterns. *Math. Geology* 39, 177–203.
- 668 Boisvert, J.B., Lyster, S., Deutsch, C.V., 2007. Constructing training images for veins and using them in multiple-point geostatistical simulation.
669 33rd International Symposium on Application of Computers and Operations Research in the Mineral Industry, APCOM 2007, E. J. Magri (ed.)
670 , 113–120.
- 671 Caers, J., Journel, A.G., 1998. Stochastic reservoir simulation using neural networks trained on outcrop data. *SPE Annual Technical Conference*
672 and Exhibition, New Orleans, LA, September 1998. Society of Petroleum Engineers. SPE paper # 49026 , 321–336.
- 673 Caers, J., Ma, X., 2002. Modeling conditional distributions of facies from seismic using neural nets. *Mathematical Geology* 34, 143–167.
- 674 Cantú-Paz, E., 1998. A survey of parallel genetic algorithms. *Calculateurs paralleles, Reseaux et Systems Repartis* 10.
- 675 Chandra, R., Dagum, L., Kohr, D., Maydan, D., McDonald, J., Menon, R., 2001. *Parallel programming in OpenMP*. Morgan Kaufmann Pub. Inc.,
676 San Francisco, CA, USA.
- 677 Culler, D., Singh, J., Gupta, A., 1998. *Parallel Computer Architecture: A Hardware/Software Approach*. Morgan Kaufmann. 1st edition. The
678 Morgan Kaufmann Series in Computer Architecture and Design.
- 679 Daly, C., 2005. Higher order models using entropy, markov random fields and sequential simulation. *Geostatistics Banff 2004*, Leuangthong, O.
680 and Deutsch, C.V., eds., , Springer , 215–224.
- 681 Daly, C., Knudby, C., 2007. Multipoint statistics in reservoir modelling and in computer vision. *Petroleum Geostatistics A*.
- 682 Datta, K., Murphy, M., Volkov, V., Williams, S., Carter, J., Olikier, L., Patterson, D., Shalf, J., Yelick, K., 2008. Stencil computation optimization
683 and auto-tuning on state-of-the-art multicore architectures, in: *Proceedings of the 2008 ACM/IEEE conference on Supercomputing*, IEEE Press,
684 Piscataway, NJ, USA.
- 685 Datta, K., Williams, S., Volkov, V., Carter, J., Olikier, L., Shalf, J., Yelick, K., 2009. Auto-tuning the 27-point stencil for multicore, in: *In Proc.*
686 *iWAPT2009: The Fourth International Workshop on Automatic Performance Tuning*.
- 687 De Jong, K.A., 1980. Adaptive system design: a genetic approach. *IEEE Transactions on Systems, Man, and Cybernetics* SMC-10, 566–574.
- 688 Deutsch, C., Wang, L., 1996. Hierarchical object-based stochastic modeling of fluvial reservoirs. *Mathematical Geology* 28, 857–880.
- 689 Deutsch, C.V., 1992. *Annealing techniques applied to reservoir modeling and the integration of geological and engineering (well test) data*. Doctoral
690 dissertation. Ph.D. thesis. Stanford University.
- 691 Deutsch, C.V., 2002. *Geostatistical Reservoir Modeling*. Oxford University Press, New York.

692 Deutsch, C.V., Journel, A.G., 1992. *GSLIB : geostatistical software library and user's guide*. Oxford University Press, New York, Oxford.

693 Eskandari, K., Srinivasan, S., 2007. Growthsim - a multiple point framework for pattern simulation. *Petroleum Geostatistics A*.

694 Faucher, C., Saucier, A., Marcotte, D., 2013. A new patchwork simulation method with control of the local-mean histogram. *Stochastic Environ-*
695 *mental Research and Risk Assessment* 27, 1–21.

696 Goldberg, D.E., 1989. *Genetic Algorithms in Search, Optimization, and Machine Learning*. Addison-Wesley.

697 Graham, S.L., Kessler, P.B., McKusick, M.K., 2004. gprof: a call graph execution profiler. *SIGPLAN Not.* 39, 49–57.

698 Guardiano, F., Srivastava, M., 1993. Multivariate geostatistics: beyond bivariate moments. *Geostatistics Troia 1*, 133–144.

699 Hennessy, J.L., Patterson, D.A., 1990. *Computer Architecture: A Quantitative Approach*. Morgan Kaufmann, San Mateo, CA.

700 Holland, J., 1975. *Adaptation in natural and artificial systems*. U. of Michigan Press.

701 Hong, S., Ortiz, J.M., Deutsch, C.V., 2008. Multivariate density estimation as an alternative to probabilistic combination schemes for data integra-
702 tion. *Geostats 2008 - Proceedings of the Eighth International Geostatistics Congress*, J.M. Ortiz and X. Emery (eds.), Gecamin Ltda., Santiago,
703 Chile 1, 197–206.

704 Intel Corporation, 2006. Fortran Compiler Use of Temporaries. <http://software.intel.com/file/20415> (Aug. 2012).

705 Intel Corporation, 2011. Intel[®] Fortran Composer XE 2011. <http://software.intel.com/en-us/articles/intel-composer-xe/> (Sep.
706 2011).

707 Krishnan, S., Journel, A.G., 2003. Spatial connectivity: From variograms to multiple-point measures. *Mathematical Geology* 35, 915–925.

708 Labarta, J., Girona, S., Pillet, V., Cortes, T., Cela, J.M., 1995. A parallel program development environment, in: *In proceedings of the 2th. Int.*
709 *Euro-Par Conference*, Springer. pp. 665–674.

710 Lyster, S., Deutsch, C.V., 2008. Mps simulation in a gibbs sampler algorithm. *Geostats 2008 - Proceedings of the Eighth International Geostatistics*
711 *Congress*, J.M. Ortiz and X. Emery (eds.), Gecamin Ltda., Santiago, Chile 1, 79–88.

712 Ortiz, J.M., 2003. Characterization of high order correlation for enhanced indicator simulation, Unpublished doctoral dissertation. Ph.D. thesis.
713 University of Alberta.

714 Ortiz, J.M., Deutsch, C.V., 2004. Indicator simulation accounting for multiple-point statistics. *Mathematical Geology* 36, 545–565.

715 Ortiz, J.M., Emery, X., 2005. Integrating multiple point statistics into sequential simulation algorithms. *Geostatistics Banff 2004*, Leuangthong,
716 O., and Deutsch, C.V., eds., Springer , 969–978.

717 Parra, A., Ortiz, J.M., 2009. Conditional multiple-point simulation with a texture synthesis algorithm. *IAMG 09 Conference*, Stanford University .

718 Peredo, O., Ortiz, J.M., 2011. Parallel implementation of simulated annealing to reproduce multiple-point statistics. *Computers & Geosciences* 37,
719 1110 – 1121.

720 Peredo, O., Ortiz, J.M., 2012. Multiple-point geostatistical simulation based on genetic algorithms implemented in a shared-memory supercom-
721 puter, in: Abrahamsen, P., Hauge, R., Kolbjørnsen, O. (Eds.), *Geostatistics Oslo 2012*. Springer Netherlands. volume 17 of *Quantitative Geology*
722 *and Geostatistics*, pp. 103–114.

723 Pycz, M.J., Strebelle, S., 2008. A showcase of event-based geostatistical models, in: Ortiz, J.M., Emery, X. (Eds.), *Geostats Oslo 2012*. Gecamin
724 Ltda., Santiago, Chile. volume 2, pp. 1143–1148.

725 Rezaee, H., Mariethoz, G., Koneshloo, M., Omid Asghari, O., 2013. Multiple-point geostatistical simulation using the bunch-pasting direct
726 sampling method. *Computers & Geosciences* 54, 293 – 308.

727 Snir, M., Otto, S., Huss-Lederman, S., Walker, D., Dongarra, J., 1998. *MPI-The Complete Reference, Volume 1: The MPI Core*. MIT Press,
728 Cambridge, MA, USA. 2nd. (revised) edition.

729 Straubhaar, J., Renard, P., Mariethoz, G., Froidevaux, R., Besson, O., 2011. An improved parallel multiple-point algorithm using a list approach.
730 *Mathematical Geosciences* , 1–24.

731 Strebelle, S., 2002. Conditional simulation of complex geological structures using multiple-point statistics. *Mathematical Geology* 34, 1–21.

732 Strebelle, S., Journel, A.G., 2000. Sequential simulation drawing structures from training images. *6th International Geostatistics Congress*, Cape
733 Town, South Africa. Geostatistical Association of Southern Africa. .

734 Tjelmeland, H., 1996. Stochastic models in reservoir characterization and Markov random fields for compact objects, Unpublished doctoral
735 dissertation. Ph.D. thesis. Norwegian University of Science and Technology.

736 Xu, W., 1996. Conditional curvilinear stochastic simulation using pixel-based algorithms. *Mathematical Geology* 28, 937–949.

737 Zanon, S., 2004. Advanced aspects of sequential Gaussian simulation. Master's thesis. University of Alberta.

738 Zhang, T., Switzer, P., Journel, A., 2006. Filter-based classification of training image patterns for spatial simulation. *Mathematical Geology* 38,
739 63–80.